Adaptive hydrophobic and hydrophilic interactions of mussel foot proteins with organic thin films

Jing Yu[a,1], Yajing Kan[a,b,1], Michael Rapp[a], Eric Danner[c], Wei Wei[d], Saurabh Das[a], Dusty R. Miller[e], Yunfei Chen[b], J. Herbert Waite[c,d], and Jacob N. Israelachvili[a,d,2]

[a]Department of Chemical Engineering, [c]Department of Molecular, Cell and Developmental Biology, and [d]Materials Research Laboratory, University of California, Santa Barbara, CA 93106; [b]Jiangsu Key Laboratory for Design and Manufacture of Micro-Nano Biomedical Instruments, Southeast University, Nanjing 211189, China; and [e]Biomolecular Science and Engineering, University of California, Santa Barbara, CA 93106

Contributed by Jacob N. Israelachvili, August 9, 2013 (sent for review June 3, 2013)

The adhesion of mussel foot proteins (Mfps) to a variety of specially engineered mineral and metal oxide surfaces has previously been investigated extensively, but the relevance of these studies to adhesion in biological environments remains unknown. Most solid surfaces exposed to seawater or physiological fluids become fouled by organic conditioning films and biofilms within minutes. Understanding the binding mechanisms of Mfps to organic films with known chemical and physical properties therefore is of considerable theoretical and practical interest. Using self-assembled monolayers (SAMs) on atomically smooth gold substrates and the surface forces apparatus, we explored the force–distance profiles and adhesion energies of three different Mfps, Mfp-1, Mfp-3, and Mfp-5, on (*i*) hydrophobic methyl (CH_3)- and (*ii*) hydrophilic alcohol (OH)-terminated SAM surfaces between pH 3 and pH 7.5. At acidic pH, all three Mfps adhered strongly to the CH_3-terminated SAM surfaces via hydrophobic interactions (range of adhesive interaction energy = −4 to −9 mJ/m^2) but only weakly to the OH-terminated SAM surfaces through H- bonding (adhesive interaction energy ≤ −0.5 mJ/m^2). 3, 4-Dihydroxyphenylalanine (Dopa) residues in Mfps mediate binding to both SAM surface types but do so through different interactions: typical bidentate H-bonding by Dopa is frustrated by the longer spacing of OH-SAMs; in contrast, on CH_3-SAMs, Dopa in synergy with other nonpolar residues partitions to the hydrophobic surface. Asymmetry in the distribution of hydrophobic residues in intrinsically unstructured proteins, the distortion of bond geometry between H-bonding surfaces, and the manipulation of physisorbed binding lifetimes represent important concepts for the design of adhesive and nonfouling surfaces.

Marine mussels are experts at wet adhesion, achieving strong and durable attachments to a variety of surfaces in their chemically heterogeneous habitat. Adhesion is mediated by a byssus, which is essentially a bundle of leathery threads that emerge from the living mussel tissue at one end and are tipped by flat adhesive plaques at the other. Byssal plaques consist of a complex array of proteins (mostly mussel foot proteins, Mfps), each of which has a distinct localization and function in the structure, but all share the unusual modified amino acid 3, 4-dihydroxyphenylalanine (Dopa) (Fig. 1).

Of the dozen or so known mussel foot proteins, Mfp-1, Mfp-3, and Mfp-5 have been shown to exhibit remarkable binding to mineral surfaces such as mica and TiO_2 (1). The versatility of mussel adhesion to surfaces with wide-ranging chemical and physical properties has inspired much research dedicated to understanding the mechanism of mussel adhesion and to developing biomimetic coatings and adhesives for wide-ranging industrial and biomedical applications, the latter including paints for coronary arteries (2), fetal membrane sealants (3), cell encapsulants (4), bone glues (5), and for securing transplants for diabetics (6).

The catecholic moiety of Dopa (Fig. 1) binds strongly to a variety of metal oxide surfaces by forming stable bidentate modes of H-bonding and metal coordination. Therefore, Dopa-containing proteins and polymers have considerable appeal as molecular coatings and glues for metal oxide surfaces. The coordination chemistry of Dopa/catecholic ligands has been studied extensively, particularly with transition metal ions (7), and is in general agreement with nanomechanical studies of tethered catechols binding to well-characterized solid surfaces. For example, atomic force microscopy tests have shown that the pull-off (adhesion) force of a single Dopa residue chemisorbed to a wet titania surface is about 1 nN (corresponding to a bond energy of ∼30 kcal/mol) and is completely reversible, as expected for a coordination complex (8). Strong adhesion forces also have been reported by recent surface forces apparatus (SFA) tests of Mfp-3 and Mfp-1 on TiO_2 substrates (9, 10).

A significant oversight in many current investigations of the mechanisms of wet adhesion is the observation that, in the natural world, surfaces such as titania and mica are not necessarily available for adhesion because they are covered by thick (often >1 μm) organic films of various types (11). How mussels contrive to adhere to such fouled surfaces is of fundamental importance, perhaps more so than their ability to adhere to the metal oxide itself. We report here on the adhesion of three Mfps to thin films (known as self-assembled monolayers, SAMs) deposited onto gold surfaces. The results suggest that in some cases Mfp–SAM adhesion is stronger than the Mfp adhesion to mica; in others, it is much weaker. These differences reveal potential strategies for promoting or inhibiting wet adhesion.

Significance

Two popular perceptions about the much-mimicked adhesion of mussels are (*i*) the adhesion depends entirely on 3, 4-dihydroxyphenylalanine (Dopa) groups (benzene derivatives with two H-bonding prongs) and (*ii*) Dopa can stick to all surfaces. This study shows that both perceptions are incorrect: using three Dopa-containing mussel foot proteins (Mfps) on two chemically different self-assembled monolayers (SAM), we found the highest adhesion on the nonpolar (i.e., hydrophobic) SAMs was exhibited by the Mfp with the most hydrophobic side chains, not the most Dopa. Furthermore, increasing the spacing between the H-bond acceptors in the SAMs prevented the double-pronged H-bonding of Dopa side chains to polar SAMs. These findings clarify the roles of hydrophobic and hydrophilic interactions in both biological and nonbiological adhesion.

Author contributions: J.Y., Y.K., Y.C., J.H.W., and J.N.I. designed research; J.Y., Y.K., M.R., E.D., W.W., S.D., and D.R.M. performed research; E.D., W.W., and D.R.M. contributed new reagents/analytic tools; J.Y., Y.K., M.R., J.H.W., and J.N.I. analyzed data; and J.Y., M.R., and J.H.W. wrote the paper.

The authors declare no conflict of interest.

[1]J.Y. and Y.K. contributed equally to this work.

[2]To whom correspondence should be addressed. E-mail: jacob@engineering.ucsb.edu.

This article contains supporting information online at www.pnas.org/lookup/suppl/doi:10.1073/pnas.1315015110/-/DCSupplemental.

A SAMs

CH_3 SAM: HS-$(CH_2)_{11}$-CH_3

OH SAM: HS-$(CH_2)_{11}$-OH

B SFA Schematic

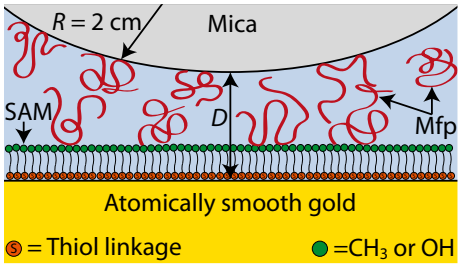

C Protein Sequences

Mfp-1: FIHNAYGSAYAGASAGAYKP
[PKISYPPTYK][PKISYPPTYK]60+
YPPSYKPKISYLPAYKPKISYPSQY

Mfp-3: GGNYYPKYKYPRGYKGGYNGYRGNY
GWNKGWKKGRWGRKYY

Mfp-5: SSEEYKGGYYPGNAYHYSGGSYHGS
GYHGGYKGKYYGKAKKYYYKYKNSG
KYKYLKKARKYHRKGYKYYGGSS

S, E = acidic amino acid
K, R, H = basic amino acid

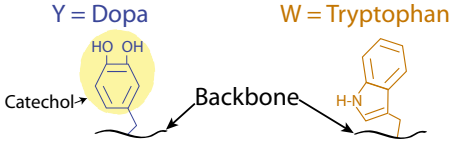

Fig. 1. Adhesive Mfps and self-assembled monolayers. (*A*) The hydrophobic CH_3-SAM (1-undecanethiol) and the hydrophilic OH-SAM (11-mercapto-1-undecanol). (*B*) Experimental setup of the asymmetric surfaces used in the SFA experiments in this study. (*C*) The amino acid sequences of Mfp-1 (sequence shown is Mcfp-1), Mfp-3 (Mcfp-3F), and Mfp-5 (Mefp-5). Italicized S residues in Mfp-5 represent phosphoserines. The Dopa catechol moiety is highlighted in light yellow.

Results

Molecularly smooth gold surfaces were prepared with a mica templating technique (12). The gold surfaces then were modified with self-assembled alkanethiol monolayers. The SAM termination directly affects the surface energy, surface chemistry, and wettability of the surfaces. To assess the adhesive versatility of the three Mfps (Mfp-1, Mfp-3, and Mfp-5) (Fig. 1) on the SAM surfaces, two different SAMs, a hydrophobic methyl-terminated SAM (CH_3-SAM) and an alcohol-terminated SAM (OH-SAM), were used in this study, giving distinctly different surface chemistries: CH_3-SAM gives a very hydrophobic surface (advancing contact angle $\theta_a \sim 110°$), whereas OH-SAM gives a hydrophilic surface ($\theta_a < 10°$) (13). These two SAMs provide two very disparate surface conditions—a very hydrophobic surface and a relatively hydrophilic surface–that mussels might encounter in their natural environment.

When separating a bare mica surface and a SAM-modified gold surface (Fig. S1), only weak adhesion forces were measured for both the methyl terminated CH_3-SAM and the alcohol terminated OH-SAM. This weak interaction is likely to arise from the relatively weak van der Waals interactions between the SAMs and mica (12). After the reference of the interaction between CH_3-SAM and bare mica was determined, picomolar amounts of Mfp-1, -3, or -5 were then added to the gap solution between the two surfaces, allowing the protein to adsorb to the mica or SAM surfaces for 20 min. After the two surfaces were brought into contact, strong adhesion forces were measured upon separation, with adhesion energies (E_{ad}) of -3.5 ± 1.0, -8.9 ± 0.2, and -6.7 ± 0.2 mJ/m^2 for Mfp-1, -3, and -5, respectively (Fig. 2*A*). Increasing the pH of the solution from 3 to 7.5 totally abolished the adhesion forces of the three Mfps between the CH_3-SAM and mica surfaces (Fig. 2*B* and Fig. S2). This loss of adhesion is expected, because the auto-oxidation of Dopa to Dopa-quinone at pH 7.5 deprives Dopa of its bidentate H-bonding anchor to the mica surface.

At pH 3 the bridging adhesions of the three Mfps between OH-SAM/mica surfaces ($E_{ad} = -0.25 \pm 0.07$, -0.37 ± 0.15, and -0.31 ± 0.02 mJ/m^2 for Mfp-1, -3, and -5, respectively) were much weaker than with the CH_3-SAM/Mfp/mica configuration (Fig. 3*A*). Similarly, all three Mfps lost the ability to bridge the two surfaces after oxidation when the solution pH was increased to 7.5 (Fig. 3*B* and Fig. S2).

A strong correlation was observed between the amount of Mfp-3 added into the gap solution between two surfaces and the measured adhesion (Fig. 4). On CH_3-SAM/mica surfaces, 80 pmol of Mfp-3 was first injected into the solution, resulting in an adhesive interaction energy (E_{ad}) of -8.8 ± 1.4 mJ/m^2. Adding 120 pmol more Mfp-3 slightly increased the adhesion to -8.9 ± 0.2 mJ/m^2. Interestingly, injecting more Mfp-3 did not enhance the adhesion further; instead, the adhesion energy leveled off at -7.3 ± 0.2 mJ/m^2 after a total of 280 pmol of Mfp-3 was injected into the solution between the CH_3-SAM and mica surfaces. A very similar correlation between the amount of Mfp-3 added and the adhesion strength was measured for the bridging adhesion of Mfp-3 across OH-SAM/mica surfaces. An E_{ad} of -0.24 ± 0.03 mJ/m^2 was measured with 80 pmol injected in the gap solution between OH-SAM and mica surfaces. The E_{ad} increased to -0.37 ± 0.13 mJ/m^2 after a total of 200 pmol Mfp-3 was added in the gap solution and decreased to only -0.23 ± 0.03 mJ/m^2 with the further addition of 280 pmol Mfp-3.

Discussion

Mfp Crowding Effect. The correlation between the amount of Mfp-3 added into the gap solution between two surfaces and the adhesion energies measured upon separation suggests that the structure of the adsorbed Mfp-3 layers on the SAM and mica surfaces is dependent on the Mfp-3 concentration. Without protein adsorption, the interactions between the SAM surface (either CH_3- or OH-terminated) are mainly van der Waals interactions (Fig. S1). When 80 pmol Mfp-3 is added to the solution between two surfaces, the surfaces are not fully covered by Mfp-3; there are large spaces between protein molecules. Every Mfp-3 molecule therefore can attach to both SAM and mica surfaces, giving rise to bridging adhesion. Further increasing the amount of Mfp-3 to 200 pmol increases the density of the adsorbed protein; however, two surfaces still are not fully covered, and therefore all the Mfp-3 molecules still can bridge across two surfaces, leading to an increase of the binding density and stronger adhesion energy. However with the addition of 280 pmol Mfp-3 both surfaces begin to be saturated with adsorbed proteins, introducing the steric repulsion between two adsorbed Mfp-3 layers. Under such conditions, some absorbed Mfp-3 molecules on one surface can repel the Mfp-3 molecules adsorbed on the other surface, reducing the chance to make bridging contact with all of the protein molecules. This steric effect therefore reduces the adhesion force despite the higher protein coverage on the surfaces. This effect is analogous to the concentration-induced microphase ordering and the corresponding steric repulsion that have been predicted in simulations of random block copolymers that have adsorbed onto two approaching surfaces (14). Additional evidence for the increasing film coverage can be seen in the increasing thickness, D_H, of the

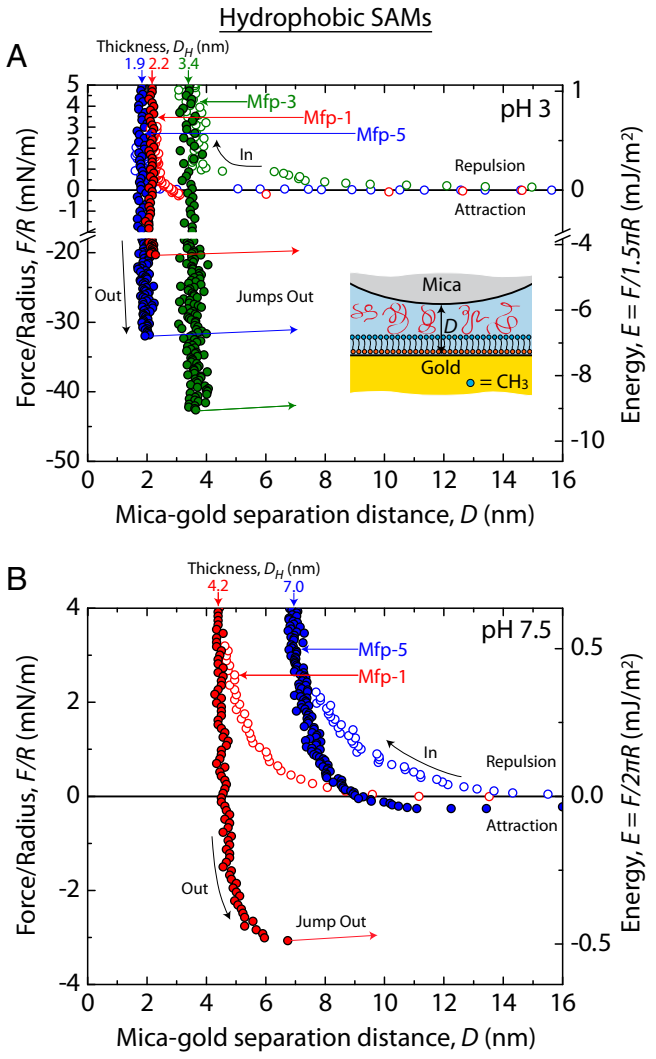

Fig. 2. Measured force–distance curves of Mfps between a hydrophobic CH_3-SAM surface and a mica surface. The measured curves correspond to ~3 pmol (~0.3 μg) of Mfp-1, ~200 pmol (~1.0 μg) of Mfp-3, or ~27 pmol (0.24 μg) of Mfp-5 injected into the gap solution between the surfaces. (*A*) Mfp-1, Mfp-3, and Mfp-5 all exhibit strong adhesion between the hydrophobic SAM and the mica surface at pH 3, and significant flattening of the contact area is observed (with fringes of equal chromatic order in the SFA). Accordingly, the adhesion energy is related to the measured force via the Johnson-Kendall–Roberts theory for the adhesion of elastic surfaces, $E_{ad} = F_{ad}/1.5\pi R$ (21). (*B*) Increasing the pH from 3 to 7.5 significantly reduces the adhesion and increases the intervening film thickness of Mfp-1 and Mfp-5. Significant flattening of the contact area was not observed for any Mfp at pH 7.5, and the adhesion energy is related to the measured force via the Derjaguin approximation (21). Data for Mfp-3 are not included because of pH-dependent protein precipitation (Fig. S2).

confined film (SAM + Mfp-3) as more Mfp-3 is added between the surfaces (Fig. 4 and Fig. S3). (D_H was taken as the absolute separation distance between the mica and gold surface at an applied load of 5 mN/m for all SAM–protein combinations.)

Mfp Interactions at the CH_3-SAM Surface. At pH 3, the strong adhesive bridging of the Mfps between a mineral (mica) surface and a hydrophobic surface indicates that the Mfps are capable of at least two distinct and concurrent adhesion mechanisms (Fig. 5*A*). At the mica interface, the commensurate spacing of the interoxygen distance of mica (0.28 nm) and the two dopa *o*-hydroxyl groups (0.29 nm) leads to bidentate H-bonding, with the dopa *o*-hydroxyls as hydrogen donors and the mica surface oxygens as hydrogen acceptors. At the CH_3-SAM interface, the uniformly hydrophobic surface does not offer the opportunity for H-bonding, covalent, or coulombic interactions to promote adhesion; in the absence of these forces, the strong adhesion at the CH_3-SAM interface must arise from hydrophobic interactions between the methyl SAM headgroups and the side chains of hydrophobic amino acid residues, as illustrated in Fig. 5*A*.

Each protein examined in this study has a unique array of hydrophobic amino acid residues that individually or synergistically can contribute to the hydrophobic adhesion to the CH_3-SAM surface. Interestingly, the most prevalent hydrophobic amino acid common to all three proteins is Dopa. The hydrophobicities of amino acids are commonly ranked according to the sign and magnitude of the free energy of transfer of an amino acid from pure

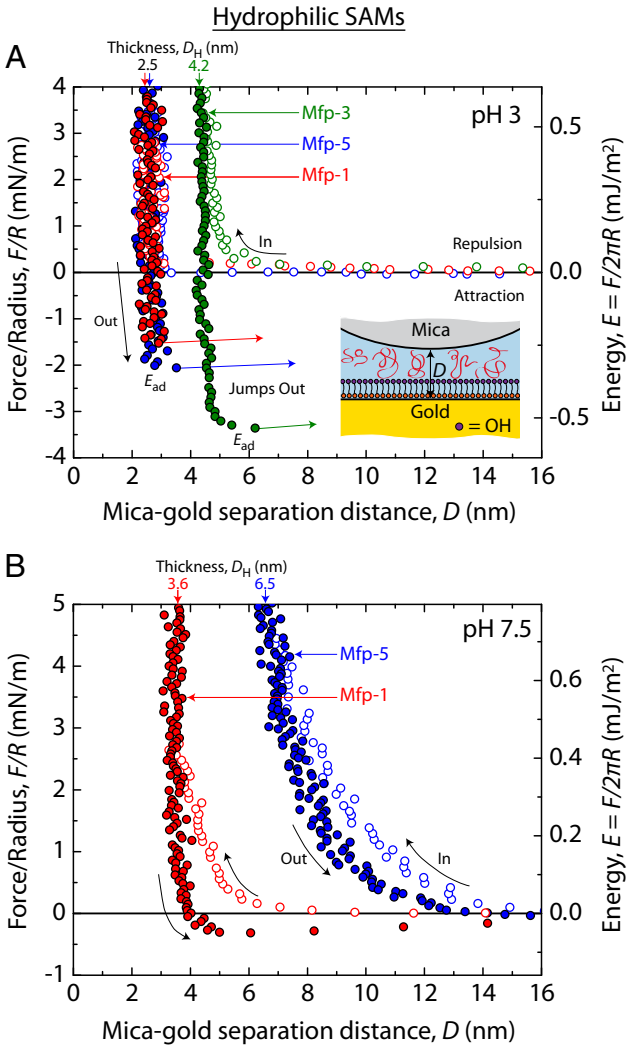

Fig. 3. Measured force–distance curves of Mfps between a hydrophilic OH-SAM surface and a mica surface. The measured curves correspond to ~3 pmol (~0.3 μg) of Mfp-1, ~200 pmol (~1.0 μg) of Mfp-3, or ~27 pmol (0.24 μg) of Mfp-5 injected into the gap solution between the surfaces. (*A*) Mfp-1, Mfp-3, and Mfp-5 all exhibit weak adhesion between the hydrophilic SAM and the mica surface at pH 3. Significant flattening of the contact area was not observed for any Mfp at pH 3, and the adhesion energy is related to the measured force via the Derjaguin approximation. (*B*) Increasing the pH from 3 to 7.5 reduces or eliminates the adhesion and increases the intervening film thickness, of Mfp-1 and Mfp-5. Data for Mfp-3 are not included because of pH-dependent protein precipitation (Fig. S2).

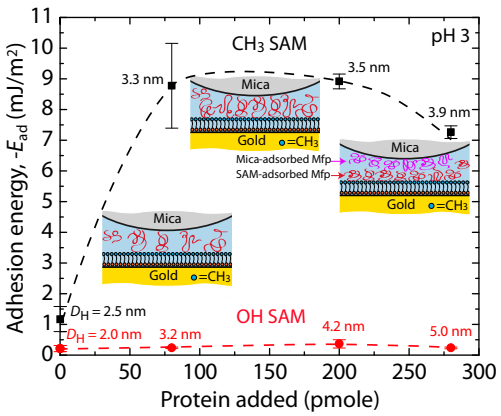

Fig. 4. The correlation between the added amount of Mfp-3 and the measured adhesion energy. The D_H values represent the total thickness of the adsorbed protein film and the SAM between the mica and gold surface at the corresponding amount of protein added. The dashed lines are provided as guides for the observed trends in adhesion energy.

ethanol to water (ΔG_t). With hydrophobic qualities similar to tyrosine [$\Delta G_{t\text{-Dopa}} = 1.8$ kcal/mol vs. $\Delta G_{t\text{-Tyrosine}} = 2.3$ kcal/mol at 25 °C (15)], Dopa is capable of interacting hydrophobically with the alkyl surface through its aromatic ring. Thus, Dopa can display Janus-like adhesive properties, forming bidentate bonds to hydrophilic mineral surfaces through its catechol group or through hydrophobic interactions at alkyl surfaces with its aromatic ring, depending on the chemistry of its neighboring surface (Fig. 5).

Other amino acid residues may contribute to hydrophobic adhesion as well. Mfp-1 contains leucine, isoleucine, and phenylalanine residues that may partition to the alkyl interface. Lysine, common to all three proteins, contains a $(CH_2)_4$ block that may contribute to the hydrophobic interaction (16). Perhaps most significantly, Mfp-3 contains three tryptophan residues, all located toward the protein's C terminus; tryptophan is the strongest partitioning amino acid with $\Delta G_{t\text{-Tryptophan}} = 3.2$ kcal/mol (15). It is hypothesized that Mfp-3′s increased adhesion over both Mfp-1 and Mfp-5 is a result of the marked asymmetric distribution of hydrophobic tryptophans along the protein length; with the predominantly hydrophobic C terminus of Mfp-3 adsorbed at the CH-SAM interface, the remainder of the molecule is more mobile to scavenge Dopa-mediated binding sites at the mica interface. This effect may be enhanced by Mfp-3′s high degree of chain flexibility (17). Preferential distribution of hydrophobic moieties toward either terminus of a peptide sequence is believed to be a favorable criterion for designing proteins with maximum adhesion between chemically heterogeneous interfaces. This notion is worthy of further investigation and may be generalized further to include the preferential distribution of any chemically specific moieties toward the end of any polymer adhesive.

The adhesion of Mfps between surfaces is adaptive. When confined between chemically asymmetric surfaces, Mfps are capable of partitioning domains of chemically specific residues to their strongest interacting surface in a strategy that lowers the protein total free energy and increases the adhesion energy (18). This process is shown through the increased adhesion energy of both Mfp-1 and Mfp-3 when confined to an asymmetric hydrophobic/mica geometry, as compared with the lower adhesion energies observed for these proteins between two symmetric mica surfaces or between two symmetric hydrophobic surfaces. Mfp-1 is a large (~108 kDa) coating protein found in the byssal cuticle and has a comparatively low Dopa concentration (15 mol%). It has been shown that Mfp-1 will coat the surface of mica; however, in doing so, it will expose its unbound—and Dopa-free—segments into solution and is incapable of bridging adhesion between two symmetric mica surfaces ($E_{ad} < -0.1$ mJ/m^2). Thus, between symmetric mineral surfaces, Mfp-1 displays its protective coating qualities rather than its bridging adhesive

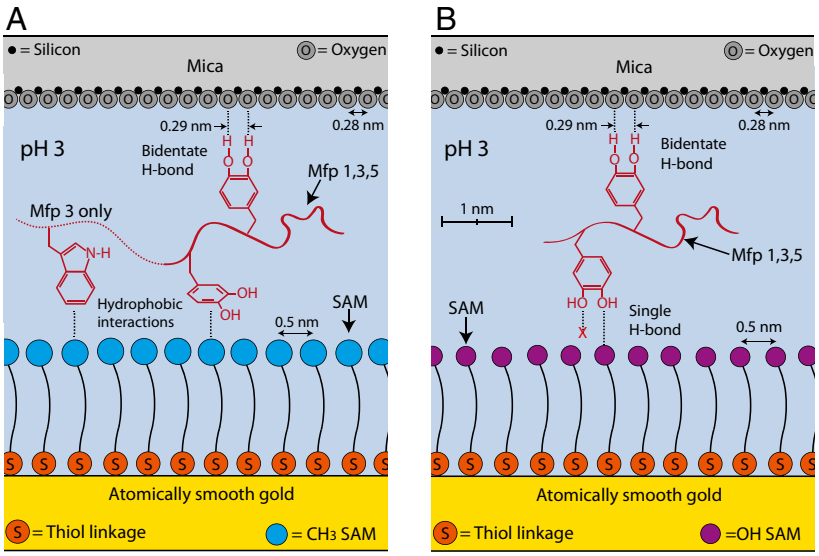

Fig. 5. The adhesion mechanisms of Mfps between mica and SAM surfaces. The sizes of the SAM molecules are drawn to scale (including headgroup size, thiol group size, chain height, and molecular spacing). The radii of the SAM headgroups and thiol groups represent the van der Waals radii of the moiety. The Dopa molecules and catechol spacing are drawn to scale. The spacing of the mica atoms is drawn to scale, and the radii of the atoms represent the ionic radii. The Mfp chains are represented schematically and are not drawn to scale. (*A*) The adhesion mechanism of Mfps between a mica surface and a CH_3-SAM surface. Although only Dopa (the most prevalent hydrophobic residue common to all three proteins) is represented as interacting at the CH_3-SAM interface for all three proteins, other contributions from hydrophobic residues certainly occur. The tryptophan-rich C terminus of Mfp-3 is represented by a solid and then dotted line. (*B*) The adhesion mechanism of Mfps between a mica surface and an OH-SAM surface. Bidentate H-bonding is not possible at the OH-SAM interface because of mismatched molecular spacing between H-bond donors and acceptors.

qualities. Likewise, when confined between two hydrophobic polystyrene surfaces, Mfp-1 is unable to bridge the surfaces and offers little adhesive potential ($E_{ad} = -0.33$ mJ/m^2 after 1 h of contact time) (10). However, when confined between the CH_3-SAM and mica interfaces, Mfp-1 displays a remarkably increased adhesion energy ($E_{ad} = -3.5 \pm 1.0$ mJ/m^2). The interfacial adhesive protein Mfp-3 also displays this same trend of increased adhesion energy between a CH_3-SAM and mica surface ($E_{ad} = -8.9 \pm 0.2$ mJ/m^2) compared with the adhesion energy between two symmetric mica surfaces ($E_{ad} = -1.2$ to -1.4 mJ/m^2) (19) or between two symmetric polystyrene surfaces ($E_{ad} = -2.7$ mJ/m^2) (10).

Mfp Interactions at the OH-SAM Surface. The minimal adhesion observed between films of both Mfp-3 and Mfp-5 to the OH-SAM surface highlights the importance of molecular geometry in bidentate-mediated surface interactions. When Mfp-3 and Mfp-5 are confined between two symmetric mica surfaces, the spacing between the catechol *o*-hydroxyl groups is commensurate with the oxygen spacing on the mica surface, which allows the formation of dopa-mediated bidentate bonds on each surface that lead to strong adhesion energies ($E_{ad,\ Mfp\text{-}3} = -1.2$ to -1.4 mJ/m^2; $E_{ad,\ Mfp\text{-}5} = -9.0$ to -13.7 mJ/m^2) (1). Strong Dopa-mediated adhesion also has been shown with Mfps on other oxide surfaces such as titania and silica that possess H- bond acceptors that lie within the reach of both dopa *o*-hydroxyl arms (8, 9, 20). However, when the spacing between the surface H-bonding groups is increased to 0.5 nm—the equilibrium headgroup spacing of the OH-SAM (Fig. 5) (21)—the catechol hydroxyls are unable to stretch to form a bidentate bond, and consequently the adhesion is reduced significantly. At the OH-SAM surface, each Dopa presumably is able to form only a single hydrogen bond with the OH-SAM headgroup. Bond lifetimes, τ, are predicted by the Bell theory: $\tau = \tau_0\ e^{-E/kT}$, where E is the bond-dissociation energy, T is temperature, k is Boltzmann's constant, and τ_0 is the average time of molecular vibrations (22). At the OH-SAM surface in aqueous solution, Dopa's single phenolic O—H—O hydrogen bond ($E_{monodentate} \sim -14$ kT) (23) will exist only $\sim 10^2$ times longer than the fleeting and promiscuous H-bonding of water to the OH-SAM surface [$E_{water\text{-}SAM} \sim -9$ kT (24)]. The transient lifetime of the monodentate hydrogen bond results in minimal Mfp adhesion observed on the OH-SAM surface in SFA force measurements, where measurements are performed over time scales much greater than the bond lifetime. This poor performance of a monodentate hydrogen bond in wet adhesion as compared with the bidentate hydrogen bond ($E_{bidentate} \sim 2E_{monodentate} \sim -28$ kT, or $\tau_{bidentate} \sim 10^6 \tau_{monodentate}$) indicates the importance of the interfacial geometry in the design of strong and robust wet adhesion to hydrophilic surfaces.

The spontaneous formation of films on surfaces, including biosurfaces, generally is thought to complicate the performance of adhesives in unpredictable ways. Our results with Mfp adhesion to SAMs suggest that subtle adjustments to film chemistry can achieve adhesion that is either stronger or weaker than the adhesion between Mfps and control surfaces. This finding has important implications for improving the performance of environmental and medical adhesives/coatings on surfaces when the chemical architecture of various natural and man-made films is known.

Experimental Procedures

Protein Purification. Mfp-1, -3, and -5 were purified as previously described (25, 26). The purified proteins were suspended in a pH 3 buffer [0.1 M acetic acid (EMD Chemicals), and 0.25 M potassium nitrate (Sigma Aldrich)]. The protein solutions were divided into small aliquots and stored at −50 °C before experiments.

Surface Preparation. Atomically smooth gold surfaces were prepared using a mica templating technique. First, a gold layer (45 nm thick) was deposited on a freshly cleaved mica sheet. The mica sheet then was glued onto a cylindrical glass disk using a UV-curable glue with the gold layer facing down to the UV glue. Then the glue was fully cured by exposing to UV light for 3 h. The mica sheet was peeled off in ethanol to reveal the atomically smooth gold surface that is predominantly single-crystalline gold with a unit cell dimension of <111> (27). Freshly cleaved gold surfaces were immersed immediately in 1 mM ethanolic solutions of the respective alkane thiols (11-mercaptoundecanol or 1-undecanethiol). The surface was kept in the thiol solution for 12 h, allowing SAM deposition, and then was rinsed thoroughly with ethanol to remove the excess alkane thiols. This technique has been shown previously to produce uniform monolayers on <111> gold surfaces with a headgroup spacing of 0.5 nm (27, 28).

SFA. The adhesion of Mfp-1, Mfp-3, and Mfp-5 on SAM surfaces was studied using an SFA 2000 (manufactured by SurForce Llc, Santa Barbara, CA) with a reported geometry (12, 29). The following buffers were used in the experiments: 0.1 M acetic acid, 0.25 M potassium nitride (pH 3); 0.016 M potassium phosphate monobasic (Mallinckrodt), and 0.084 M potassium phosphate dibasic (EMD Chemicals) (pH 7.5). Milli-Q water (MilliporeA) was used for all glassware cleaning and solution preparation.

ACKNOWLEDGMENTS. This work was supported by the MRSEC Program of the National Science Foundation (NSF) under Award DMR 1121053, National Institute of Health Grant R01-DE018468, and an NSF Graduate Research Fellowship (M.R.).

1. Lee BP, Messersmith PB, Israelachvili JN, Waite JH (2011) Mussel-inspired adhesives and coatings. *Ann Rev Mater Res* 41:99–132.
2. Kastrup CJ, et al. (2012) Painting blood vessels and atherosclerotic plaques with an adhesive drug depot. *Proc Natl Acad Sci USA* 109(52):21444–21449.
3. Haller CM, et al. (2011) Mussel-mimetic tissue adhesive for fetal membrane repair: A standardized ex vivo evaluation using elastomeric membranes. *Prenat Diagn* 31(7):654–660.
4. Yang SH, et al. (2011) Mussel-inspired encapsulation and functionalization of individual yeast cells. *J Am Chem Soc* 133(9):2795–2797.
5. Winslow BD, Shao H, Stewart RJ, Tresco PA (2010) Biocompatibility of adhesive complex coacervates modeled after the sandcastle glue of Phragmatopoma californica for craniofacial reconstruction. *Biomaterials* 31(36):9373–9381.
6. Brubaker CE, Kissler H, Wang LJ, Kaufman DB, Messersmith PB (2010) Biological performance of mussel-inspired adhesive in extrahepatic islet transplantation. *Biomaterials* 31(3):420–427.
7. Sedó J, Saiz-Poseu J, Busqué F, Ruiz-Molina D (2013) Catechol-based biomimetic functional materials. *Adv Mater* 25(5):653–701.
8. Lee H, Scherer NF, Messersmith PB (2006) Single-molecule mechanics of mussel adhesion. *Proc Natl Acad Sci USA* 103(35):12999–13003.
9. Yu J, et al. (2013) Adhesion of mussel foot protein-3 to TiO2 surfaces: The effect of pH. *Biomacromolecules* 14(4):1072–1077.
10. Lu QY, et al. (2013) Adhesion of mussel foot proteins to different substrate surfaces. *J R Soc Interface* 10(79):20120759.
11. Stewart RJ, Ransom TC, Hlady V (2011) Natural Underwater Adhesives. *J Polym Sci, B, Polym Phys* 49(11):757–771.
12. Valtiner M, Donaldson SH, Jr., Gebbie MA, Israelachvili JN (2012) Hydrophobic forces, electrostatic steering, and acid-base bridging between atomically smooth self-assembled monolayers and end-functionalized PEGolated lipid bilayers. *J Am Chem Soc* 134(3):1746–1753.
13. Bain CD, et al. (1989) Formation of monolayer films by the spontaneous assembly of organic thiols from solution onto gold. *J Am Chem Soc* 111(1):321–335.
14. Gutman L, Chakraborty AK (1994) Surface-Induced Ordering for Confined Random Block-Copolymers. *J Chem Phys* 101(11):10074–10091.
15. Nozaki Y, Tanford C (1971) The solubility of amino acids and two glycine peptides in aqueous ethanol and dioxane solutions. Establishment of a hydrophobicity scale. *J Biol Chem* 246(7):2211–2217.
16. Creighton TE (1993) *Proteins: Structures and Molecular Properties* (W. H. Freeman, New York), 2nd Ed.
17. Hwang DS, Waite JH (2012) Three intrinsically unstructured mussel adhesive proteins, mfp-1, mfp-2, and mfp-3: Analysis by circular dichroism. *Protein Sci* 21(11):1689–1695.
18. Even MA, Wang J, Chen Z (2008) Structural information of mussel adhesive protein Mefp-3 acquired at various polymer/Mefp-3 solution interfaces. *Langmuir* 24(11):5795–5801.
19. Yu J, et al. (2011) Mussel protein adhesion depends on interprotein thiol-mediated redox modulation. *Nat Chem Biol* 7(9):588–590.
20. Frank BP, Belfort G (2002) Adhesion of Mytilus edulis foot protein 1 on silica: Ionic effects on biofouling. *Biotechnol Prog* 18(3):580–586.
21. Yang YC, Chang TY, Lee YL (2007) Adsorption behavior of 11-mercapto-1-undecanol on Au(111) electrode in an electrochemical system. *J Phys Chem C* 111(10):4014–4020.

22. Israelachvili JN (2011) *Intermolecular and Surface Forces* (Academic, Burlington, MA), 3rd Ed.
23. Feller D, Feyereisen MW (1993) Ab-initio study of hydrogen-bonding in the phenol water-system. *J Comput Chem* 14(9):1027–1035.
24. Jorgensen WL (1981) Quantum and statistical mechanical studies of liquids. 10. Transferable intermolecular potential functions for water, alcohols, and ethers - application to liquid water. *J Am Chem Soc* 103(2):335–340.
25. Waite JH, Qin XX (2001) Polyphosphoprotein from the adhesive pads of Mytilus edulis. *Biochemistry* 40(9):2887–2893.
26. Waite JH (1995) Precursors of quinone tanning: Dopa-containing proteins. *Methods Enzymol* 258:1–20.
27. Chai L, Klein J (2007) Large area, molecularly smooth (0.2 nm rms) gold films for surface forces and other studies. *Langmuir* 23(14):7777–7783.
28. Strong L, Whitesides GM (1988) Structures of self-assembled monolayer films of organosulfur compounds adsorbed on gold single-crystals - electron-diffraction studies. *Langmuir* 4(3):546–558.
29. Israelachvili J, et al. (2010) Recent advances in the surface forces apparatus (SFA) technique. *Rep Prog Phys* 73(3):036601.